Demonstration of Longitudinal Power Profile Estimation using Commercial Transceivers and its Practical Consideration

Junho Chang, Choloong Hahn, Xuefeng Tang, Tianyu Zhao, Wing Chau Ng, Zhiping Jiang*

Ottawa Research Centre, Huawei Technologies Canada, 303 Terry Fox Drive, Ottawa, Canada, zhiping.jiang@huawei.com

Abstract *We demonstrate the correlation-based longitudinal power profile estimation of an optical link using commercial transceivers and discuss the impact of practical constraints such as a limited data size, erroneous templates, and implementation complexity.*

Introduction

Monitoring the physical properties of an optical link is crucial for ensuring reliable and effective network operations [1]. Currently, there are two prevalent approaches to accomplish this task: 1) utilizing additional monitoring equipment such as the optical time-domain reflectometers (OTDR) or optical spectrum analysers (OSA) installed throughout the link, or 2) extracting information from digital signal processing (DSP) at the receiver side. However, the former method incurs increased costs and/or complexity (e.g., out-of-band signal), while the latter approach only provides cumulative values for the entire link. Recently, a novel method has been proposed that utilizes the nonlinear Kerr effect of optical fibres to enable longitudinal monitoring without requiring additional hardware [2]. Using only the received signal, this method can measure the various physical properties of multi-span optical links. Previous literatures have demonstrated its capability in estimating longitudinal power profiles, identifying fibre-types [3], and localizing link anomalies such as losses [3-5], multi-path interferences [6], faulty amplifiers [7,8], and off-centred optical filters [8]. However, these attempts were conducted offline, typically using high-speed sampling oscilloscopes with a sufficient number of samples and sampling rate.

In this work, we demonstrate the use of commercial transceivers for longitudinal power profile estimation (PPE) for the first time to our knowledge, where either analog-to-digital convertor (ADC)-buffer samples or demodulated output symbols obtained directly from the transceivers are used. We show the estimated power profile of a 12-span optical link by averaging size-limited data sets with only 1 sample per symbol. Additionally, we discuss potential inaccuracies commonly observed in correlation-based PPE methods along with practical constraints. By leveraging the accessibility of ADC buffer or demodulated symbols in most commercialized transceivers, we present a practical example of how PPE can be adopted to existing systems, which is an important step toward the productization of this technique.

Principle of PPE using correlation templates

In general, PPE relies on the uniqueness of local Kerr nonlinear distortion imposed on a signal waveform during its propagation. Fig. 1 shows the block diagram of a PPE method using correlation templates [9]. We may assume the signal waveform at location z_i is $E(z_i,t) = \sqrt{P(z_i)}u(z_i,t)$ where $P(z_i)$ and $u(z_i,t)$ are the local power and normalized waveform at location z_i, respectively. In the regular perturbation model, the nonlinear distortion at the location is $E_{\mathrm{NL}}(z_i,t) = -j\gamma E(z_i,t)|E(z_i,t)|^2$ [10]. The total received waveform after chromatic dispersion compensation (CDC) is then expressed as $u_{\mathrm{R}}(t) = u(0,t) + \sum_{i=1}^{N} H(E_{\mathrm{NL}}(z_i,t), -CD_i)$, where H is an operator to apply dispersion and CD_i is the accumulated dispersion from Tx to z_i. For PPE, we generate correlation templates, $u_{\mathrm{t}}(z_i,t) = -j\gamma\hat{u}(z_i,t)|\hat{u}(z_i,t)|^2$, using a reference waveform, $\hat{u}(t)$, which is obtained after decision. As the templates emulate the normalized version of the nonlinear waveform at each location, the power profile, $P(z)$, can be calculated from their

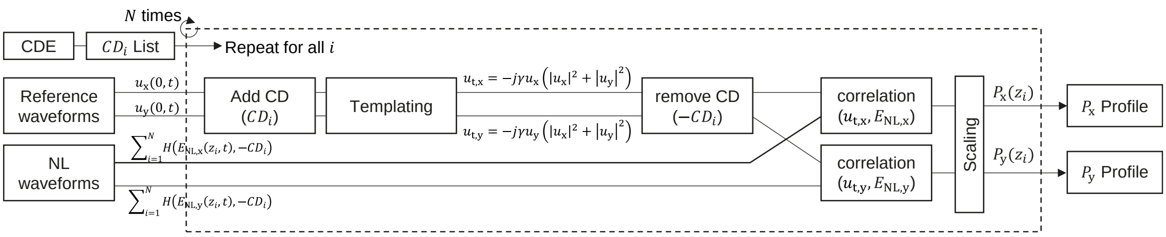

Fig. 1: Block diagram of correlation-template-based PPE function

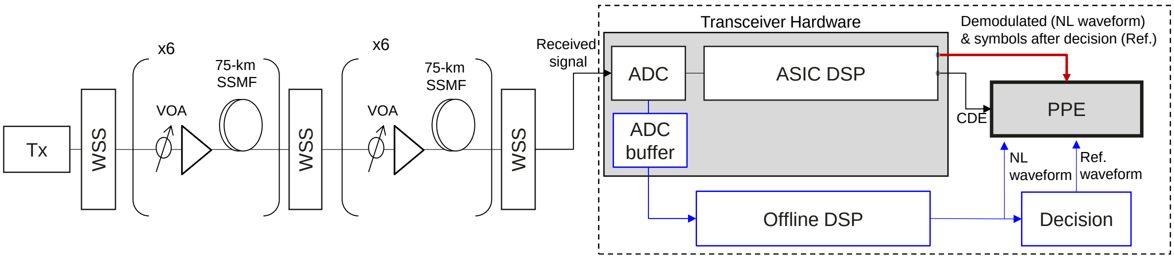

Fig. 2: Experimental setup with a schematic of the data flow for PPE (blue line: ADC buffer, red line: demodulated symbols). CDE: chromatic dispersion estimation, WSS: wavelength-selective switch, VOA: variable optical attenuator

correlation [2,9].

Demonstration of PPE using commercial transceivers

To demonstrate our PPE using a commercial product, we used a transceiver line card supporting a 68-Gbaud dual-polarization QPSK or 16QAM signal. The configuration of our data extraction/processing at the Rx is illustrated in the dashed box of Fig. 2. The received signal was sampled by 96-Gsa/s ADCs and then processed with standard DSPs for data recovery. The transceiver that we used offered two access points for data extraction: 1) ADC buffer, and 2) the direct output of demodulated symbols. The size of ADC buffer was ~32k samples per tributary while only a 768-long consecutive demodulated symbols could be extracted at a time. We tested both cases in this work and, if necessary, used fast DSPs with training patterns to obtain demodulated symbols from ADC buffer data. Fig. 2 shows the experimental setup for PPE of a 12-span link. The signal was transmitted over the dispersion-uncompensated link consisting of 75-km long standard SMFs, and we set the span launch power to be ~ 5 dBm. The number of CD steps, N, and the step size were 1000 and 15.2 ps/nm, respectively. We repeatedly ran the PPE function for different CD_i to calculate the correlation intensity at each location. Fig. 3(a) shows the estimated power profile (solid line) together with the theoretical one (dashed line). The total number of symbols

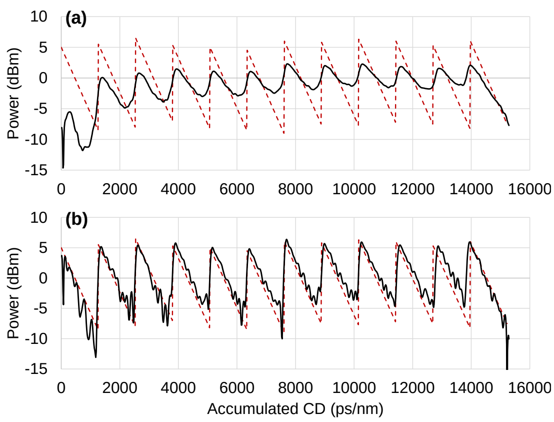

Fig. 3: Estimated power profile (a) before and (b) after correction (solid line: PPE, dashed line: theoretical profile)

used for averaging was ~850k. The results suggest that the estimated profile might be useful for a quick span length or fibre type identification but there are still a large discrepancies from the theoretical profile.

Correction of spatial response and low-PAPR

The inaccuracy of the results is because, as pointed out in [11], the correlation-based PPEs are inherently affected by the spatial response of the correlation function. A template $u_t(z_i, t)$ is not always uniquely correlated to the nonlinear distortion waveform at location z_i, $E_{\mathrm{NL}}(z_i, t)$. Moreover, in the low-CD region, the low peak-to-average power ratio (PAPR) of the signal may cause a weak nonlinear waveform which leads to an underestimation of the power profile. To address this issue, we define $C_{\mathrm{NL}}(i,k) = corr\left(u_t(z_i,t),\, u_t(z_k,t)\right)$ as a correction factor. Fig. 4(a) shows the values of $C_{\mathrm{NL}}(i,k)$ as a function of k for several different i. The correlation is most noticeable when $k = i$ as expected; however, the correlation width is

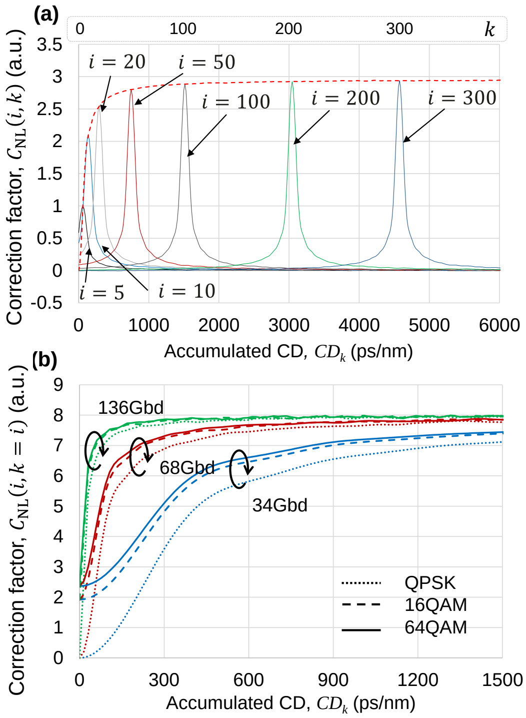

Fig. 4: (a) Spatial response and relative correlation intensity, $C_{\mathrm{NL}}(i,k)$, at different locations, and (b) the dependency of the peak correlation intensity (i.e., $i = k$) on signal's properties

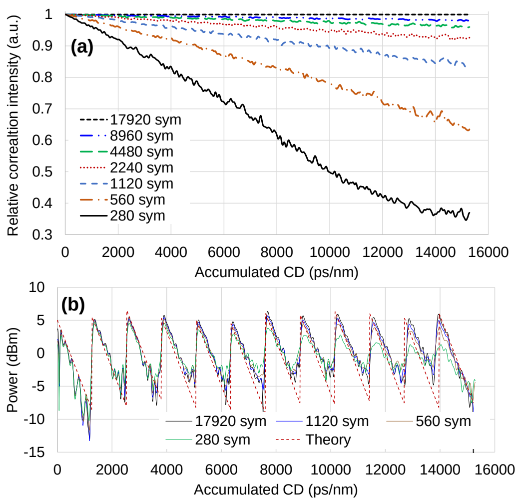

Fig. 5: (a) Reduction of correlation between a full-length data set and segmented data sets, and (b) the underestimation of PPE using an insufficient data length

shown to be ~130 ps/nm (equivalently ~7.5 km). It should be also noted that the peak value of correlation diminish when the accumulated CD is not sufficient at the beginning of the link. This indicates that $C_{\mathrm{NL}}(i,k)$ incorporates the effects of both low PAPR and the spatial response. The values of $C_{\mathrm{NL}}(i,k)$ are highly dependent on the signal, as shown in Fig. 4(b). From the results, we can expect the underestimation of PPE for the first few spans becomes less problematic as we increase the baud rate and format order. To retrieve the actual power profile, we used the regularized least square method. If we formulate $C_{\mathrm{NL}}(i,k)$ to be a $N \times N$ matrix, M, the power profile after correction, P_{post}, can then be obtained from that before correction, P_{pre}, as follow: $P_{\mathrm{post}} = (M'M + \lambda \mathrm{I})/(M'P_{\mathrm{pre}})$, where λ is the regulation factor. Fig. 3(b) shows the estimated power profile after correction, showing a good agreement with the theoretical one.

Discussion on practical constraints

We discuss major constraints that must be considered in practical scenarios.

1) Impact of data size

At the edge of a data block, it is not feasible to create a perfect nonlinear waveform template due to the lack of information outside the data block. Thus, the use of non-consecutive data sets with a limited size can be problematic especially in the case of large CD such as ultra-long-haul and/or L-band transmission. Fig. 5(a) shows the relative correlation intensity between the template of a 17920-symbol-long data set and that of the divided (and shorter) data sets with various lengths. It clearly shows the correlation is weakened as we reduce the size of the data sets, resulting in the underestimation of PPE in the high-CD region as depicted in Fig. 5(b). This

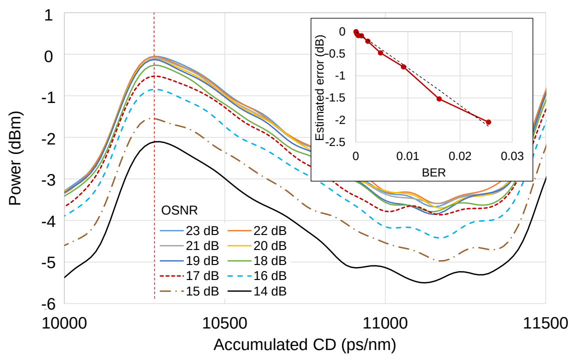

Fig. 6: Impact of the erroneous templates on PPE

could be partially compensated by using the results in Fig. 5(a) or applying a weighted-window to the data sets.

2) OSNR or BER of the received signal

When creating templates, it may not always possible to use a perfect reference waveform (e.g., post-forward error correction (FEC)). In such case, a pre-FEC data has to be used. However, the pre-FEC data often differs from the actual transmitted data and it may weaken the correlation. Fig. 6 shows the estimated power profiles while varying the received OSNR. Note that we used the data before correction here to minimize the effect of noise. As expected, the estimated power decreases as the OSNR is reduced. The inset shows the power offset required to eliminate this effect as a function of the bit-error rate (BER).

3) Low-complexity implementation of PPE

The implementation complexity of PPE heavily depends on the complexity of CDC. A multiple times of CDC, often with a large amount, are required to complete a set of correlation for all locations along the link. It is imperative to simplify the CDC process and reduce the overall complexity. One way is to use symbol-rate data rather than oversampled one (as we did in this work) for PPE. The required number of taps for CDC can be reduced by ~36% when the oversampling rate is 1 instead of 1.25 [12]. In addition, the use of lookup tables of the correction factor, $C_{\mathrm{NL}}(i,k)$, would be beneficial as it is deterministic and depends on signal properties such as format, baud rate, and pre-distortions.

Conclusions

We have shown the feasibility of using commercial transceivers for PPE. By utilizing only data that are easily accessible from any commercial product, we have demonstrated the PPE for a 12-span link. We have also highlighted several factors that might impact the accuracy of PPE. With careful consideration of these factors, we believe that PPE can be used in a various applications even with existing products.

References

[1] Y Pointurier, “Design of low-margin optical networks”, Journal of Optical Communications and Networking, vol. 9, no. 1, pp. A9-A17, 2017.
DOI: 10.1364/JOCN.9.0000A9.

[2] T. Tanimura, S. Yoshida, K. Tajima, S. Oda, and T. Hoshida, “Fiber-longitudinal anomaly position identification over multi-span transmission link out of receiver-end signals”, Journal of Lightwave Technology, vol. 38, no. 9, pp. 2726-2733, 2020.
DOI: 10.1109/JLT.2020.2984270.

[3] T. Sasai, M. Nakamura, S. Okamoto, F. Hamaoka, S. Yamamoto, E. Yamazaki, A. Matsushita, H. Nishizawa, and Y. Kisaka, “Simultaneous detection of anomaly points and fiber types in multi-span transmission links only by receiver-side digital signal processing”, in *Proceedings Optical Fiber Communication Conference*, paper Th1F.1, 2020.
DOI: Not available yet.

[4] A. May, F. Boitier, A. C. Meseguer, J. U. Esparza, P. Plantady, A. Calsat, and P. Layec, "Longitudinal power monitoring over a deployed 10,000-km link for submarine systems," in *Proceedings Optical Fiber Communication Conference*, paper Tu2G.3, 2023.
DOI: Not available yet.

[5] I. Kim, O. Vassilieva, R. Shinzaki, M. Eto, S. Oda, and P. Palacharla, "Robust longitudinal power profile estimation in optical networks using MMSE with complex scaling factor," in *Proceedings Optical Fiber Communication Conference*, paper W4H.6, 2023.
DOI: Not available yet.

[6] C. Hahn, J. Chang, and Z. Jiang, “Localization of reflection Induced multi-path-interference over multi-span transmission link by receiver-side digital signal processing”, in *Proceedings Optical Fiber Communication Conference*, paper Th1C.3, 2022.
DOI: Not available yet.

[7] M. Sena, R. Emmerich, B. Shariati, C. Santos, A. Napoli, J. K. Fischer, and R. Freund, “DSP-based link tomography for amplifier gain estimation and anomaly detection in C+ L-band systems”, Journal of Lightwave Technology, vol. 40, no. 11, pp. 3395-3405, 2022.
DOI: 10.1364/JLT.40.003395.

[8] T. Sasai, M. Nakamura, E. Yamazaki, S. Yamamoto, H. Nishizawa, Y. Kisaka, “Digital longitudinal monitoring of optical fiber communication link”, Journal of Lightwave Technology, vol. 40, no. 8, pp. 2390-2408, 2022.
DOI: 10.1109/JLT.2021.3139167.

[9] C. Hahn, and Z. Jiang, “On the spatial resolution of location-resolved performance monitoring by correlation method”, in *Proceedings Optical Fiber Communication Conference*, paper W1H.2, 2023.
DOI: Not available yet.

[10] A. Bononi, P. Serena, “An alternative derivation of Johannisson's regular perturbation model,” published on arXiv,
http://arxiv.org/abs/1207.4729, July 19th, 2012.
DOI: 10.48550/arXiv.1207.4729.

[11] T. Sasai, E. Yamazaki, M. Nakamura, and Y. Kisaka, “Closed-form expressions for fiber-nonlinearity-based longitudinal power profile estimation methods”, in Proceedings European Conference on Optical Communication, paper Tu1D.6, 2022.
DOI: Not available yet.

[12] R. Kudo, T. Kobayashi, K. Ishihara, Y. Takatori, A. Sano, and Y. Miyamoto, “Coherent optical single carrier transmission using overlap frequency domain equalization for long-haul optical systems”, Journal of Lightwave Technology, vol. 27, no. 16, pp. 3721-3728, 2009.
DOI: 10.1109/JLT.2009.2024091.